Quantitative Parameters from OCT Angiography in Patients with Diabetic Retinopathy and in Those with Only Peripheral Retinopathy Compared with Control Participants

Hogg, R. E., Wright, D. M., Dolz-Marco, R., Gray, C., Waheed, N., Teussink, M., Naska, T. K., Perais, J., Das, R., Quinn, N., Bontzos, G., Nicolaou, C., Annam, K., Young, I., Kee, F., McGuinness, B., McKay, G., Macgillivray, D. T., & Chakravarthy, U. (2021). Quantitative Parameters from OCT Angiography in Patients with Diabetic Retinopathy and in Those with Only Peripheral Retinopathy Compared with Control Participants. *Ophthalmology Science*, *1*(2), Article 100030. https://doi.org/10.1016/j.xops.2021.100030

Published in:
Ophthalmology Science

Document Version:
Publisher's PDF, also known as Version of record

AMERICAN ACADEMY OF OPHTHALMOLOGY®

Quantitative Parameters from OCT Angiography in Patients with Diabetic Retinopathy and in Those with Only Peripheral Retinopathy Compared with Control Participants

Ruth E. Hogg, PhD,[1] David M. Wright, PhD,[1] Rosa Dolz-Marco, MD,[2] Calum Gray, PhD,[3] Nadia Waheed, MD,[4] Michel M. Teussink, PhD,[2] Timos Naskas, PhD,[1] Jennifer Perais, BSc(Hons),[1] Radha Das, MD, PhD,[5] Nicola Quinn, PhD,[1] George Bontzos, MD,[6] Constantinos Nicolaou, MD,[1] Kaushik Annam, MD,[7] Ian S. Young, MD, PhD,[1] Frank Kee, MD, PhD,[1] Bernadette McGuiness, MD, PhD,[1] Gareth Mc Kay, MD, PhD,[1] Tom MacGillivray, PhD,[3] Tunde Peto, MD, PhD,[1] Usha Chakravarthy, MD, PhD[1]

Purpose: To describe the differences in a range of quantitative OCT angiography (OCTA) metrics across early stages of diabetic retinopathy (DR), providing robust effect estimates as well as sensitivity and specificity.

Design: Cross-sectional study with population-based sampling.

Participants: Four hundred forty-one eyes from 296 individuals: 328 control eyes (no diabetes mellitus [DM] and no DR), 55 eyes with DM and no DR, and 58 eyes with early nonproliferative DR.

Methods: Multimodal retinal imaging included color fundus photography, color Optomap ultra-widefield imaging, and spectral-domain OCT (Spectralis OCT2; Heidelberg Engineering GmbH) with the OCTA module. All images were graded for the presence and severity of DR features. OCTA images were assessed manually for inclusion based on quality. Binary OCTA metrics were assessed after 3-dimensional projection artifact removal including from the nerve fiber layer vascular plexus, superficial vascular plexus (SVC), and deep vascular plexus (DVC) by Early Treatment Diabetic Retinopathy Study (ETDRS) grid, foveal avascular zone (FAZ) area, FAZ minimum and maximum diameter, perimeter length, and circularity.

Main Outcome Measures: Diabetes mellitus and DR status and presence or absence of DR in the retinal periphery.

Results: The reduction in vessel densities in participants with DM and manifest DR compared with control participants tended to be twice that of those with DM, but no DR, compared with control participants. Some evidence of spatial heterogeneity in vessel reductions was found in those yet to develop DR, whereas those with manifest DR had significant reductions across the ETDRS grid. The FAZ perimeter and circularity were impacted most significantly by DM, and those with DR showed decreased multispectral fractal dimensions compared with control participants. Eyes with peripheral DR had reduced vessel density compared with those with DM and no DR only in the superior outer, temporal inner, and temporal outer regions in the DVC and SVC. The area under the receiver operating characteristic curve ranged between 0.48 and 0.73.

Conclusions: Significant differences in OCTA metrics can be found in those with DM before manifest DR using commercially available equipment with minimal image postprocessing. Although diagnostic performance was poor, these metrics may be useful for measuring change over time in clinical trials. *Ophthalmology Science 2021;1:100030 © 2021 Published by Elsevier Inc. on behalf of the American Academy of Ophthalmology. This is an open access article under the CC BY-NC-ND license (http://creativecommons.org/licenses/by-nc-nd/4.0/).*

Supplemental material available at www.ophthalmologyscience.org.

Diabetic retinopathy (DR) is the most common complication of diabetes mellitus (DM) and is a leading cause of sight loss worldwide.[1] Traditionally, DR has been considered to be a vasculopathy mainly affecting the arteriolar and capillary components of the retinal vascular bed.[2] Initially, fluorescein angiography with videography was used to study vascular morphologic features, retinal blood flow, and transit times and clearly showed morphologic and functional DM-induced pathologic features.[3,4] Over the years, additional methodologies were developed, including laser Doppler velocimetry,[5] color Doppler imaging,[6] Doppler OCT,[7] and adaptive optics scanning laser ophthalmoscopy.[8] These

https://doi.org/10.1016/j.xops.2021.100030
ISSN 2666-9145/21

highly specialist devices were used almost exclusively within research settings, yet some of the findings in early DR literature were conflicting.[9] More recently, the complex interplay between neuronal components of the retina and its circulatory bed arising as a consequence of the metabolic perturbations of DM has entered the scientific dialog driven by the better detection of the earliest manifestations resulting from improvements in noninvasive retinal imaging. OCT angiography (OCTA) now offers a more widely applicable method for investigating the integrity of blood flow in health and disease by using changes in the reflectance signal between repeated B-scans at a specific location to construct a map of blood flow. Because bulk motion from the patient is eliminated from the signal by eye tracking or image processing, the main source of motion between repeated scans is assumed to represent erythrocyte movement in the choroidal and retinal blood vessels.[10] It offers comparable qualitative and quantitative microvascular details to adaptive optics scanning laser ophthalmoscopy and fluorescein angiography, but with the capability of applying sophisticated real-time image processing algorithms and 3-dimensional representations. All traditional clinical signs of nonproliferative DR such as microaneurysms, intraretinal microvascular abnormalities, areas of nonperfusion, and neovascularization, are visible on OCTA,[11] with additional capacity to localize these features precisely to specific vascular layers[12] based on segmentation of the retinal layers. Most commercial devices also offer various quantitative measures such as vessel density, vessel tortuosity, fractal dimension and area, and dimensions of the foveal avascular zone (FAZ), which could be helpful in the identification and staging of DR.[11]

Many groups have sought to characterize the early vascular manifestations of DR before the development of clinical features in patients with DM using technologies that have been available for many years (color fundus photography, OCT, fluorescein angiography). OCT angiography has been used to compare retinal vascular morphologic features in patients with DM without DR with those with manifest DR and with control participants without DM, with reported lower retinal vessel densities in the macula among patients with DM.[9,13] Palochak et al[9] undertook a retrospective analysis of OCTA images obtained from the TIME-2b Study and showed the presence of vascular abnormalities in both the superficial capillary plexus and deep capillary plexus, as well as reporting that FAZ area and temporal peripapillary vessel density were predictors for DR progression during 12 months of follow-up. Because the retinal capillary bed can exhibit changes resulting from aging and is affected by conditions such as cardiovascular disease and hypertension,[14] carefully designed prospective studies incorporating a substantial control population are necessary to ensure appropriate accounting for variation resulting from known and unknown factors. Furthermore, substantial interest exists in using quantitative parameters from OCTA as clinical trial end points in intervention trials,[15] but accurate spatial characterization of such parameters along with age and gender-related effects will be needed to ensure precise sample size calculations. To the best of our knowledge, this type of population-based data currently are not available. Also, concerns exist regarding OCTA-specific artifacts such as those related to projection, local signal loss, and eye motion that lead to limited reliability of vessel segmentation and erroneous metrics that have hampered the adoption and use of quantitative parameters in both clinical practice and trials.[16]

To address these gaps in knowledge, we exploited the ongoing study of aging in Northern Ireland (the Northern Ireland Cohort for the Longitudinal Study of Aging [NICOLA]), in which we were able to design prospectively and to include acquisition of OCTA data in specific groups of participants. Participants were recruited using unbiased community-based sampling, and all underwent multimodal retinal imaging, with a subsample invited to return for additional functional tests and retinal imaging, including OCTA. A contemporaneous clinic-based sample with DR also was recruited because it was apparent that manifest DR was present in a low proportion of participants in the NICOLA sample. The aims of this study were (1) to provide robust estimates of differences quantitative OCTA metrics depending on DM and DR status and presence or absence of DR in the retinal periphery and (2) to assess diagnostic performance of each metric.

Methods

Participants

Data were collected as part of a prospective study of early imaging and functional biomarkers of DR and age-related macular degeneration in NICOLA. The NICOLA study is a population-based epidemiologic study of aging that involved a computer-assisted home interview followed by a health assessment at the Northern Ireland Clinical Research Facility. The health assessment included an eye component comprising best-corrected visual acuity, intraocular pressure measurement, autorefraction, and multimodal retinal imaging (color fundus photography, ultra-widefield imaging, and spectral-domain OCT). Retinal images were assessed systematically by trained graders within the Network of Ophthalmic Reading Centres UK for the presence of various common retinal diseases. Based on the retinal grading, the following participants were invited to return for a second visit comprising a battery of further retinal imaging and functional tests, including OCTA: (1) no sign of retinal disease and (2) a self-reported a history of DM at either the home interview or health assessment.

Ethical approval for the study was obtained from the School of Medicine, Dentistry and Biomedical Sciences Ethics Committee, Queen's University Belfast (reference, 12/23; reference, 16.37v2). The study adhered to the tenets of the Declaration of Helsinki, and all participants gave informed written consent.

Retinal Imaging

Participants underwent pupil dilation using 1% tropicamide before retinal imaging. Color fundus photography of the disc and macula with 50° field of view was performed using a Canon CX-1 Digital Fundus Camera (Canon USA, Inc). Color ultra-widefield images centered on the fovea were captured using the Optomap Panoramic 200Tx scanning laser ophthalmoscope (Optos PLC).

Image capture of multicolor, spectral-domain OCT, and OCTA imaging was performed with the Spectralis HRA+OCT2 (Heidelberg Engineering GmbH). Training was provided by the

manufacturer both before and at regular intervals throughout the data acquisition phase. Fovea-centered multicolor images (768 × 768 pixels) had a 30° field of view and a resolution of approximately 11 μm per pixel. Each macular OCT volume scan comprised 61 horizontal B-scan lines with a spacing of approximately 125 μm on a 30° × 25° (horizontal × vertical) scan angle and was acquired using TruTrack Active Eye Tracking, for automatic real-time averaging of 8 scans per B-scan. Fovea-centered OCTA images were acquired on a 10° × 10° scan angle, automatic real-time (ART) 7 and 512 × 512 pixels at an isotropic resolution of 5.7 μm. The onboard clinical software was used for automated retinal layer segmentation of 11 boundaries in the OCT and OCTA scans. Following the manufacturer's definition of the retinal vascular plexuses, the superficial vascular complex (SVC) was delimited by the retinal nerve fiber layer and a 17-μm offset anterior to the inner plexiform layer (IPL) boundaries, whereas the deep vascular complex (DVC) was delimited by a 17-μm offset anterior to the inner plexiform layer and the outer plexiform layer boundaries.

Multimodal Diabetic Retinopathy Grading

Disc and macula color images were assessed for characteristic DR features and then staged using the national screening for DR system for England, Wales, and Northern Ireland into 4 levels: none (R0), background (R1), preproliferative (R2), and proliferative (R3). Maculopathy and photocoagulation scars were graded as absent (M0, P0) or present (M1, P1). Ultra-widefield retinal images underwent transformation using Optos stereographic projection software (ProView), which considers the optical imaging system and the ocular geometry to map each pixel to a consistent spherical geometry. This allows accurate representation of retinal features throughout the image, compensating for distortions resulting from the retinal curvature and enabling subsequent measurements made on the images in pixels to be converted to millimeter equivalents.[17] Inaccurately projected images resulting from quality, gaze angle, or both were reprojected manually using Image J software (National Institutes of Health), finding the x- and y- coordinates of the fovea. Optos V2 Vantage Dx Review version 2.5.0.135 was used to view the images, and DR was graded using the system outlined by Silva et al.[18,19] Diabetic retinopathy features were recorded within the Early Treatment Diabetic Retinopathy Study (ETDRS) 7 fields, and the retina outside this area was divided into 5 peripheral fields. For this analysis, presence of DR features only in the area outside the ETDRS 7 fields was recorded as peripheral DR only.

OCT Angiography Image Quality Grading and Postprocessing

OCT angiography images were viewed using Spectralis software version 6.9 and assessed individually for quality by 1 grader (R.E.H.) and a subset checked by another grader (U.C.) and classified according to the proportion of the microvasculature in the SVC slab that was seen clearly and not obscured by artifact, using this quality scale: grade 5, 100%; grade 4, 99% to 80%; grade 3, 80% to 60%; grade 2, 60% to 40%; and grade 1, less than 40%. Images that were classified as grades 4 and 5 were imported using the manufacturer supplied prototype OCTA Analytics software (Spectralis viewing module version 6.12.4.710) for OCTA postprocessing and analysis of microvascular density by various quantitative parameters. Grade 3 was considered borderline and reviewed individually before extraction of OCTA metrics. Grade 1 and 2 images were excluded. Examples from each grade are shown in Figure 1.

OCTA quality scores produced by the device indicate the average signal-to-noise ratio of the OCTA volume, but do not account for, for example, focus errors, suboptimal optical alignment, and erroneous layer segmentation. The quality scores therefore were insufficient to determine overall image quality as evidenced by several cases in which blink, movement, and segmentation artifacts, or otherwise poor visibility of the microvasculature, were reasons for exclusion, despite high quality scores (Supplemental Fig 1).

Using the OCTA Analytics software, images were postprocessed using a proprietary 3-dimensional projection artifact removal algorithm, which incorporates a 3-dimensional vessel shape estimate and corrects for 3-dimensional projection tails of OCTA signal into the retinal tissue.

Vessel Density Assessment

We exported grid-wise the quantitative OCTA parameters of each vascular slab according to the fovea-centered modified ETDRS 123 grid, which uses ring diameters of 1, 2, and 3 mm and measures 9 sectors. The prototype exploratory software uses proprietary algorithms to provide a large range of vessel density parameters. For comparison purposes, we selected only the binary vessel density parameter and the nerve fiber layer vascular plexus (NFLVP), SVC, and DVC slabs. The binary metric is the most consistent with binarized vessel density parameters used in previous publications because it classifies whether the A-scan in the vascular slab includes a vessel.

Fractal Dimensions and Foveal Avascular Zone Characteristics

Custom designed software written in MATLAB (MathWorks) was used to analyze the superficial vascular layer OCTA images. We used the multifractal analysis method previously described by Stosic and Stosic.[20] In multifractal analysis, the image first is binarized to segment the vessels. The retinal vasculature is characterized as a spectrum of dimensions at different scales, with fractal dimension being a metric ranging between 1 and 2, with higher values reflecting increased complexity of a vascular network. For the Fourier fractal analysis method, the image was transformed to the Fourier spectrum and plotted against the frequency in a log−log scale. No prior segmentation was performed, and the technique was applied directly to the grayscale image. The FAZ region was segmented and FAZ area, minimum and maximum diameter, and the perimeter length were measured (Supplemental Fig 2). Foveal avascular zone circularity was estimated using the formula: circularity $= 4\pi(\text{area} / \text{perimeter}^2)$, where a value of 1.0 indicates a perfect circle and a value approaching 0.0 indicates an increasingly elongated polygon.

Statistical Analysis

Associations between OCT Angiography Metrics and Diabetes Mellitus and Diabetes Retinopathy Status. Analyses were conducted in R software version 3.6.2 (R Foundation for Statistical Computing). The quantitative parameters were reported as means and standard deviations. To estimate differences in OCTA metrics between DM and DR groups, a hierarchical linear regression was fitted for each metric in each slab. In each regression, the OCTA metric was the response variable with DM and DR status as the main predictor and compared with those without diabetes (control participants). Interaction terms between DM and DR status and ETDRS 123 sectors 1, 2, and 3 were specified as fixed effects to estimate simultaneously within each region the mean value among

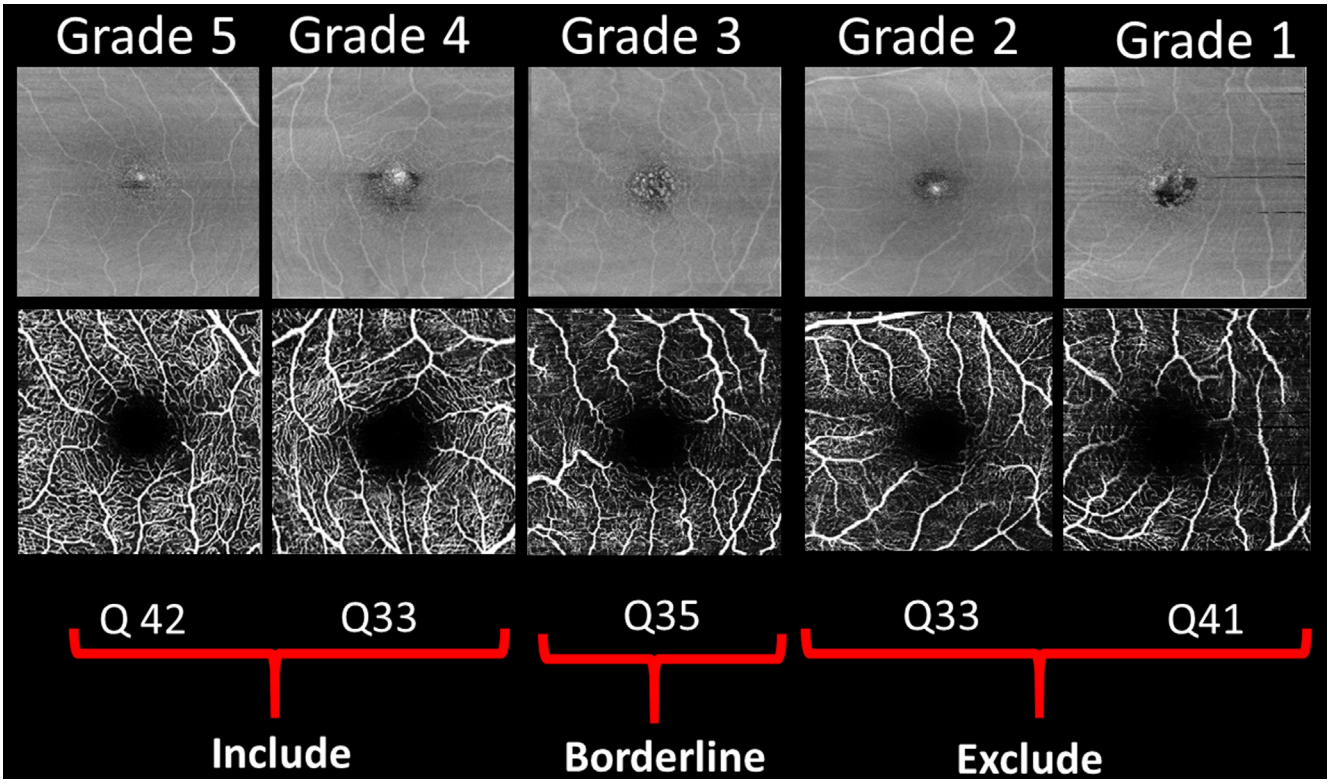

Figure 1. Example images of quality (Q) assessment of macular OCT angiography scans.

control participants and the differences associated with DM and DR status.

Random effects for the intercept were fitted for eyes nested within participants to allow for correlations among regions within eyes and between eyes within individuals. Analysis was conducted first with borderline cases excluded, and then included trends were similar in both analyses. Therefore, they were retained to increase the power. Two sets of models were fitted, the first adjusting for age and sex alone, with fixed effects for sex using linear and quadratic functions of age, and a second set additionally adjusted for potential covariates (spherical equivalent, hypertension history, and smoking status).

Additional models were fitted to investigate whether associations existed between OCTA metrics and presence of DR in the periphery among those with DM. A comparison was made between those with DM and no DR (anywhere) and those with DR in the periphery only (detected using ultra-widefield imaging).

Diagnostic Performance of OCT Angiography. Diagnostic performance of each OCTA metric was assessed for 2 classification tasks: control participants versus patients with DM and no DR, and control participants versus patients with DR. For each task, the OCTA metric was the sole predictor used in the classification. Area under the receiver operating characteristic curve (AUC) statistics were calculated from receiver operating characteristic curves. The AUC was calculated by slab and ETDRS region for the binary vessel metric and globally for the other metrics (e.g., FAZ area).

Results

In total of 686 eyes were imaged with OCTA. Exclusions included 15 eyes because of other pathologic features, 83 eyes because of poor-quality images, and 147 eyes because of presence of early or intermediate age-related macular degeneration. The final sample consisted of 441 eyes from 296 individuals. Table 1 shows the clinical characteristics of 3 groups: control participants, patients with DM and no DR, and patients with DR. There were 328 control eyes (no diabetes and no retinal disease), 55 eyes with DM and no DR, and 58 eyes with DR. All except 3 eyes with DR showed mild nonproliferative DR without diabetic macular edema. See Figure 2 for examples of the 3 classes of participants.

Analysis was focused on 3 slabs: NFLVP, SVC, and DVC. Distribution of OCTA metrics within each of these slabs was unimodal within each ETDRS region (Fig 3). For both the SVC and DVC, the central region, C0, showed markedly lower values compared with other regions because it includes the FAZ with a bimodal distribution and a heavy tail to the left.

Associations between OCT Angiography Metrics and Diabetes Mellitus and Diabetes Retinopathy Status

Table 2 provides the mean, standard deviation, and selected quantiles for the NFLVP, SVC, and DVC for the binarized vessel metric. Hierarchical linear regression for comparisons of vessel density between control participants and the 2 DM groups, without DR and with DR, are shown in Table 3. Statistically significant differences between control participants and patients with DM and no DR were few and

Table 1. Cohort Characteristics

Characteristic	All	Control Group	Diabetes Mellitus and No Diabetic Retinopathy	Nonproliferative Diabetic Retinopathy	Peripheral Diabetic Retinopathy Only*
No. of eyes	441	328	55	58	11
No of individuals	296	222	39	44	9
Age, yrs	66.1 ± 8.1	65.6 ± 8.3	68.6 ± 7	66.2 ± 7.5	68.3 ± 5.2
HbA1c (%)	6.1 ± 1.4	5.5 ± 0.3	7.2 ± 1.3	7.8 ± 2.4	7.2 ± 2
Duration of diabetes (mos)	120 (60–180)	N/A	96 (60–180)	120 (60–180)	120 (54–144)
Diabetes type					
I			1 (1.8)	7 (12.1)	0 (0.0)
II			43 (78.2)	51 (87.9)	11 (100.0)
Unknown			11 (20.0)	0 (0.0)	0(0.0)
Spherical equivalent	0.7 ± 2	0.7 ± 2	1 ± 2	0.8 ± 2.4	0.1 ± 2.3
Sex					
Male	167 (37.9)	149 (45.4)	6 (10.9)	12 (20.7)	1 (9.1)
Female	274 (62.1)	179 (54.6)	49 (89.1)	46 (79.3)	10 (90.9)
History of hypertension					
Negative	249 (56.5)	218 (66.5)	18 (32.7)	13 (22.4)	1 (9.1)
Positive	192 (43.5)	110 (33.5)	37 (67.3)	45 (77.6)	10 (90.9)
Smoking status					
Never	232 (52.6)	182 (55.5)	27 (49.1)	23 (39.7)	4 (36.4)
Former	176 (39.9)	125 (38.1)	22 (40.0)	29 (50.0)	7 (63.6)
Current	21 (4.8)	9 (2.7)	6 (10.9)	6 (10.3)	0 (0.0)
Unknown	12 (2.7)	12 (3.7)	0 (0.0)	0 (0.0)	0 (0.0)

HbA1c = hemoglobin A1c; N/A = not applicable.
Data are presented as mean±standard deviation, median (interquartile range), or no. (%).
*Subgroup of diabetes retinopathy group.

effect sizes were small, but the associations were in the expected direction of decreased density (−0.3% to −4.7% for SVC) in those with DM. Vessel densities were significantly lower (i.e., negative values for comparison estimates) in eyes from the DR group across most of the ETDRS regions in both DVC and SVC slabs. Most ETDRS inner sectors (1, 2, and 3) in the DVC showed reduced vascular density compared with control participants. In the

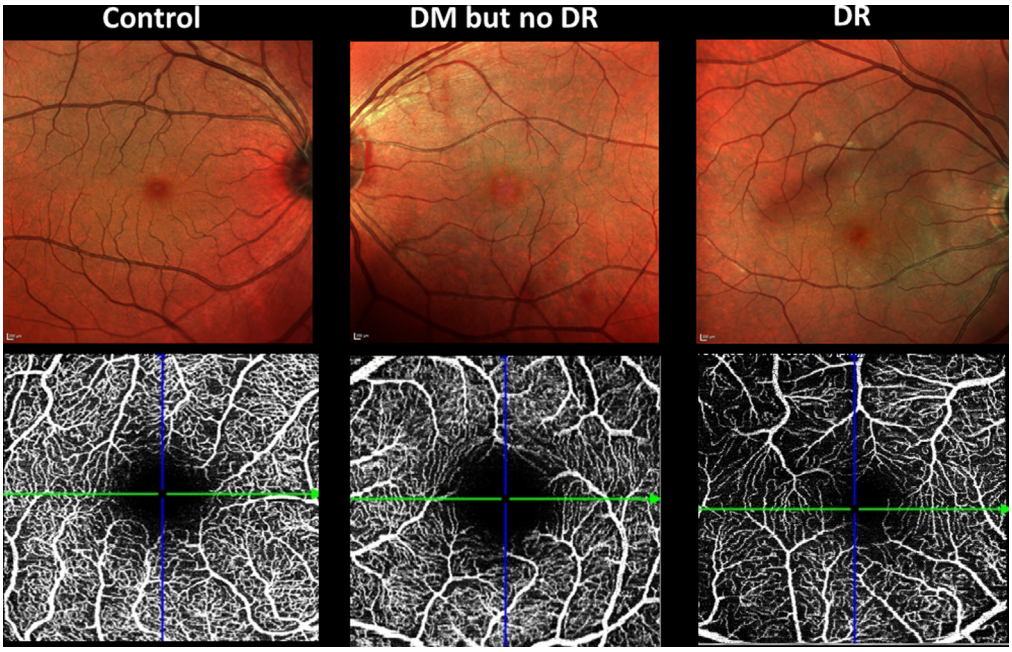

Figure 2. Example images from the 3 groups: control participants (no diabetes mellitus [DM] and no diabetic retinopathy [DR]), DM but no DR, and DR. **Top row**, Confocal multicolor images. **Bottom row**, OCT angiography showing the superficial vascular complex.

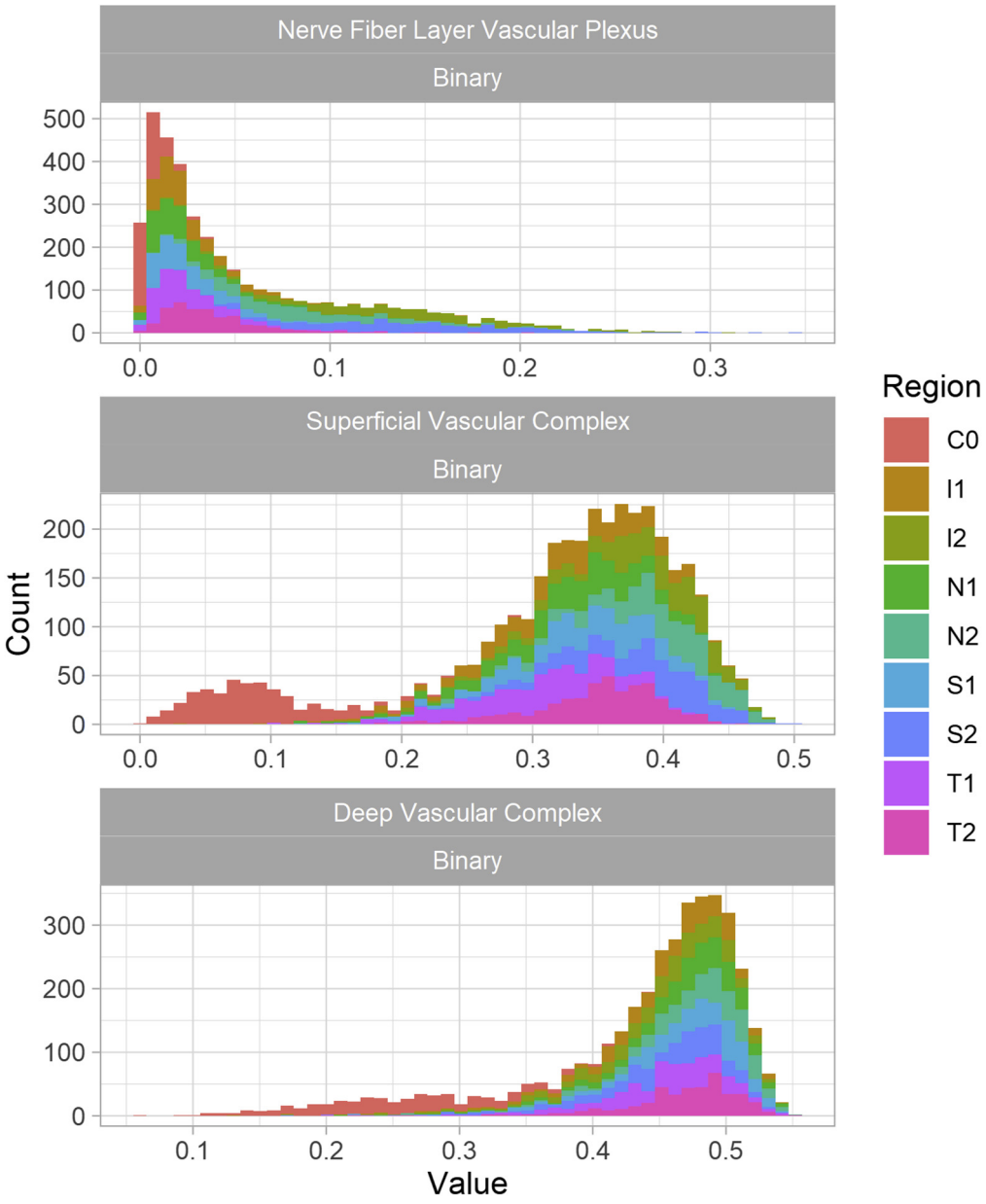

Figure 3. Graphs showing the distribution of OCT angiography vessel density according to layer and Early Treatment Diabetic Retinopathy Study segment.

NFLVP slab, only 2 regions (I2 and S2) showed lower vessel densities in the DR group compared with the control group. The magnitude of differences between eyes with DR versus those of control participants was at least twice that of the difference between control participants and the DM with no DR group (−6.7% to −9.7% vs. −4.7 to 1.4 in SVC). In the DM without DR group of eyes, the outer sectors of the ETDRS grid showed significant differences in the inferior and nasal regions (Table 3).

Table 4 shows the association between OCTA FAZ characteristics and whole image fractal metrics and DM and DR status. Compared with control participants, significant differences in FAZ perimeter length and circularity were seen in eyes from patients with DM and no DR and from patients with DR. No significant differences were seen for FAZ area or the minimum or maximum diameter. Both DM groups showed smaller FAZ perimeter when compared with control participants, whereas FAZ circularity was greater even in the fully adjusted models for both groups. Fourier average fractal dimension was increased in patients with DM with no DR compared with control participants, consistent with a more complex arrangement of vessels, and was sparser and less dense in those with DR. Only the DM with no DR versus control association was significant in the fully adjusted model for average fractal dimension. After full adjustment, only those with DR showed a significantly sparser multispectral fractal dimension compared with control participants.

Table 2. Distribution of OCT Angiography Binary Metric for Selected Slabs and Regions

Slab	Region	Diabetes Mellitus and Diabetic Retinopathy Status	Mean	Standard Deviation	Quality Score				
					2.5%	25%	50%	75%	97.5%
Nerve fiber layer vascular plexus	C0	Control	0.006	0.007	0.000	0.001	0.004	0.008	0.026
	C0	DM and no DR	0.007	0.009	0.000	0.002	0.005	0.009	0.028
	C0	DR	0.008	0.008	0.000	0.003	0.006	0.010	0.028
	I1	Control	0.027	0.023	0.003	0.012	0.021	0.035	0.094
	I1	DM and no DR	0.026	0.018	0.006	0.011	0.023	0.039	0.068
	I1	DR	0.027	0.021	0.002	0.013	0.020	0.036	0.072
	I2	Control	0.139	0.054	0.043	0.103	0.134	0.170	0.257
	I2	DM and no DR	0.124	0.063	0.016	0.082	0.113	0.167	0.239
	I2	DR	0.128	0.054	0.013	0.100	0.122	0.166	0.220
	N1	Control	0.023	0.019	0.003	0.010	0.019	0.030	0.076
	N1	DM and no DR	0.029	0.026	0.003	0.011	0.021	0.037	0.091
	N1	DR	0.025	0.028	0.003	0.010	0.019	0.027	0.092
	N2	Control	0.087	0.044	0.023	0.055	0.079	0.110	0.194
	N2	DM and no DR	0.082	0.047	0.023	0.046	0.066	0.108	0.193
	N2	DR	0.078	0.037	0.031	0.052	0.072	0.094	0.157
	S1	Control	0.027	0.021	0.003	0.012	0.022	0.035	0.088
	S1	DM and no DR	0.033	0.021	0.005	0.016	0.031	0.047	0.072
	S1	DR	0.029	0.023	0.005	0.012	0.020	0.038	0.087
	S2	Control	0.142	0.055	0.048	0.104	0.138	0.176	0.252
	S2	DM no DR	0.138	0.056	0.048	0.098	0.139	0.173	0.258
	S2	DR	0.132	0.054	0.049	0.092	0.127	0.165	0.245
	T1	Control	0.025	0.023	0.004	0.012	0.019	0.032	0.091
	T1	DM and no DR	0.032	0.026	0.004	0.014	0.026	0.044	0.074
	T1	DR	0.030	0.030	0.001	0.009	0.019	0.039	0.112
	T2	Control	0.037	0.025	0.008	0.019	0.031	0.048	0.096
	T2	DM and no DR	0.045	0.027	0.010	0.022	0.039	0.064	0.099
	T2	DR	0.040	0.032	0.007	0.020	0.032	0.048	0.121
Superficial vascular complex	C0	Control	0.089	0.045	0.020	0.058	0.083	0.112	0.200
	C0	DM and no DR	0.078	0.049	0.017	0.041	0.066	0.113	0.178
	C0	DR	0.093	0.056	0.024	0.053	0.084	0.116	0.255
	I1	Control	0.328	0.060	0.202	0.289	0.335	0.371	0.419
	I1	DM and no DR	0.307	0.062	0.160	0.274	0.311	0.350	0.405
	I1	DR	0.302	0.077	0.147	0.245	0.313	0.365	0.403
	I2	Control	0.382	0.057	0.240	0.354	0.387	0.425	0.462
	I2	DM and no DR	0.382	0.051	0.258	0.364	0.398	0.414	0.440
	I2	DR	0.363	0.060	0.234	0.325	0.375	0.408	0.443
	N1	Control	0.332	0.054	0.217	0.301	0.340	0.368	0.420
	N1	DM and no DR	0.307	0.064	0.179	0.267	0.315	0.353	0.411
	N1	DR	0.304	0.068	0.150	0.279	0.322	0.348	0.410
	N2	Control	0.400	0.046	0.296	0.375	0.405	0.432	0.470
	N2	DM and no DR	0.382	0.050	0.286	0.350	0.394	0.417	0.454
	N2	DR	0.371	0.057	0.247	0.337	0.379	0.414	0.452
	S1	Control	0.340	0.054	0.228	0.310	0.346	0.379	0.429
	S1	DM and no DR	0.326	0.056	0.216	0.280	0.336	0.369	0.412
	S1	DR	0.316	0.065	0.176	0.278	0.328	0.370	0.402
	S2	Control	0.383	0.053	0.262	0.350	0.395	0.421	0.462
	S2	DM and no DR	0.373	0.053	0.273	0.335	0.386	0.413	0.455
	S2	DR	0.356	0.061	0.245	0.316	0.356	0.402	0.451
	T1	Control	0.305	0.051	0.211	0.269	0.308	0.340	0.392
	T1	DM and no DR	0.282	0.057	0.129	0.251	0.298	0.315	0.374
	T1	DR	0.283	0.064	0.147	0.242	0.285	0.343	0.372
	T2	Control	0.353	0.046	0.245	0.330	0.359	0.385	0.428
	T2	DM and no DR	0.348	0.047	0.256	0.318	0.353	0.386	0.418
	T2	DR	0.323	0.057	0.197	0.285	0.336	0.364	0.399
Deep vascular complex	C0	Control	0.263	0.069	0.132	0.217	0.263	0.312	0.397
	C0	DM and no DR	0.240	0.065	0.130	0.191	0.231	0.280	0.358
	C0	DR	0.255	0.079	0.117	0.195	0.247	0.307	0.408
	I1	Control	0.456	0.053	0.321	0.431	0.468	0.493	0.527
	I1	DM and no DR	0.445	0.049	0.360	0.420	0.451	0.477	0.508
	I1	DR	0.422	0.062	0.275	0.413	0.432	0.457	0.502
	I2	Control	0.444	0.061	0.278	0.415	0.458	0.488	0.525
	I2	DM and no DR	0.444	0.044	0.354	0.417	0.450	0.475	0.505

(*Continued*)

Table 2. (Continued.)

Slab	Region	Diabetes Mellitus and Diabetic Retinopathy Status	Mean	Standard Deviation	Quality Score				
					2.5%	25%	50%	75%	97.5%
	I2	DR	0.425	0.061	0.265	0.397	0.435	0.466	0.513
	N1	Control	0.473	0.045	0.354	0.458	0.483	0.502	0.530
	N1	DM and no DR	0.446	0.059	0.280	0.433	0.462	0.478	0.510
	N1	DR	0.444	0.054	0.326	0.418	0.453	0.482	0.516
	N2	Control	0.482	0.044	0.377	0.463	0.492	0.510	0.536
	N2	DM and no DR	0.459	0.057	0.296	0.442	0.472	0.492	0.522
	N2	DR	0.450	0.045	0.350	0.430	0.454	0.481	0.509
	S1	Control	0.473	0.046	0.360	0.451	0.485	0.504	0.533
	S1	DM and no DR	0.454	0.046	0.349	0.427	0.466	0.490	0.516
	S1	DR	0.446	0.058	0.305	0.416	0.460	0.487	0.513
	S2	Control	0.455	0.052	0.325	0.432	0.468	0.489	0.519
	S2	DM and no DR	0.437	0.053	0.318	0.400	0.456	0.476	0.515
	S2	DR	0.422	0.061	0.296	0.385	0.432	0.474	0.500
	T1	Control	0.457	0.043	0.364	0.433	0.463	0.486	0.525
	T1	DM and no DR	0.439	0.053	0.303	0.424	0.454	0.474	0.505
	T1	DR	0.427	0.053	0.300	0.400	0.432	0.465	0.504
	T2	Control	0.471	0.041	0.372	0.454	0.479	0.496	0.525
	T2	DM and no DR	0.464	0.037	0.390	0.444	0.467	0.493	0.512
	T2	DR	0.443	0.058	0.287	0.421	0.454	0.479	0.508

DM = diabetes mellitus; DR = diabetic retinopathy.

Associations between Central OCT Angiography Metrics and Presence of Diabetes Retinopathy in the Periphery

Of those with DR present, 11 showed peripheral disease only. Eyes with peripheral DR showed only reduced binarized vessel density compared with those with DM and no DR in the S2, T1, and T2 regions in the DVC and SVC (Table 5).

Diagnostic Performance of OCT Angiography

Area under the receiver operating characteristic curve statistics calculated from receiver operating characteristic curves ranged from 0.48 to 0.73 when comparing control participants versus patients with DM and no DR and control participants versus patients with DR, with the latter comparison performing slightly better in general (Tables 3 and 4). Within each ETDRS region, the highest AUC values were derived from measurements of the DVC, followed by the SVC. Measurements from the NFLVP performed no better than a random classifier in most regions for both comparisons.

Discussion

This study demonstrated that spatially specific quantitative differences in OCTA vessel density can be identified between control participants and those with DM even before the onset of clinically overt DR. The measurements were made without prior manual segmentation using a prototype OCTA Analytics software package on a commonly used imaging platform demonstrating easy clinical applicability. Although the magnitude of change in vessel density was modest, the decrease in eyes without overt DR remained detectable, showing the potential for OCTA-based vessel density quantification as an outcome measure in prophylaxis and interventional trials. Although other studies have reported quantitative changes in this disease, this study reports effect size differences between control participants versus patients with DM and no DR, and control participants versus patients with early DR after projection artefact removal using the device manufacturer's OCTA Analytics software while correcting for multiple covariates. We showed that the differences between patients with DR and control participants is approximately twice that between control participants and patients with DM and no DR. Longitudinal studies will be required to determine the significance of these findings.

Vessel density analysis has been reported in patients with diabetes with different retinopathy stages.[21,22] In our study, patients with DR showed lower values for the OCTA metrics across most of the central ETDRS grid sectors when analyzing the DVC. Regarding the SVC, fewer sectors showed significant differences, and none on the NFLVP. These results in general are agreement with those of previous publications.[21,22] Early detection of ophthalmoscopically nonvisible neurovascular changes with OCTA has been tested in patients with diabetes before the first clinical signs of DR appear.[23–25] In this context, a recent meta-analysis showed that a decrease in the vascular density values could be detected on OCTA images in eyes without overt DR.[23] However, it is notable that our study showed that the differences in vessel density between groups is small, detecting a reduction in vessel density of approximately 5% in the patients with DM and no DR and of 10% in the patients with DM and DR.

Characterization of the FAZ is one of the most commonly reported metrics in studies evaluating OCTA and DR.[26–33] Most studies have used small control groups, which limits their efforts to adjust for the population-based

Table 3. Associations between OCT Angiography Binary Metric and Diabetes Mellitus and Diabetic Retinopathy Status

	Control Group vs. Diabetes Mellitus and No Diabetic Retinopathy Group*									Control Group vs. Diabetic Retinopathy Group								
Metric	*C0*	*I1*	*I2*	*N1*	*N2*	*S1*	*S2*	*T1*	*T2*	*C0*	*I1*	*I2*	*N1*	*N2*	*S1*	*S2*	*T1*	*T2*
Nerve fiber layer vascular plexus																		
Reference	0.002	0.023	0.135	0.019	0.083	0.023	0.138	0.021	0.033	0.002	0.023	0.135	0.019	0.083	0.023	0.138	0.021	0.033
Comparison	0.002	−0.002	−0.019	0.005	−0.008	0.005	−0.008	0.006	0.007	0.002	−0.001	−0.012	0.001	−0.009	0.000	−0.017	0.004	0.003
Difference (%)	0.0	−8.7	−14.1	26.3	−9.6	21.7	−5.8	28.6	21.2	0.0	−4.3	−8.9	5.3	−10.8	0.0	−12.3	19.0	9.1
P value	0.670	0.690	**0.001**	0.410	0.150	0.410	0.193	0.270	0.220	0.650	0.840	**0.033**	0.830	0.100	0.940	**0.003**	0.490	0.590
AUC (95% CI)	0.55 (0.47, 0.63)	0.51 (0.43, 0.60)	0.58 (0.48, 0.67)	0.56 (0.47, 0.64)	0.55 (0.46, 0.63)	0.60 (0.52, 0.68)	0.48 (0.39, 0.56)	0.60 (0.52, 0.69)	0.59 (0.51, 0.68)	0.59 (0.51, 0.67)	0.49 (0.41, 0.58)	0.55 (0.46, 0.63)	0.52 (0.44, 0.60)	0.55 (0.47, 0.63)	0.49 (0.40, 0.57)	0.55 (0.47, 0.64)	0.49 (0.40, 0.59)	0.52 (0.44, 0.60)
Superficial vascular complex																		
Reference	0.096	0.335	0.389	0.338	0.407	0.347	0.390	0.311	0.360	0.096	0.335	0.389	0.338	0.407	0.347	0.390	0.311	0.360
Comparison	−0.003	−0.012	0.010	−0.016	−0.009	−0.005	−0.001	−0.013	0.005	0.009	−0.031	−0.026	−0.030	−0.031	−0.031	−0.035	−0.027	−0.035
Difference (%)	−3.1	−3.6	2.6	−4.7	−2.2	−1.4	−0.3	−4.2	1.4	9.4	−9.3	−6.7	−8.9	−7.6	−8.9	−9.0	−8.7	−9.7
P value	0.730	0.130	0.224	**0.047**	0.250	0.570	0.880	0.120	0.57	0.290	**<0.001**	**0.001**	**<0.001**	**<0.001**	**<0.001**	**<0.001**	**<0.001**	**<0.001**
AUC (95% CI)	0.59 (0.50–0.68)	0.60 (0.52–0.68)	0.49 (0.42–0.57)	0.61 (0.53–0.70)	0.60 (0.53–0.68)	0.57 (0.48–0.65)	0.56 (0.48–0.64)	0.61 (0.53–0.68)	0.53 (0.45–0.62)	0.50 (0.41–0.58)	0.59 (0.50–0.68)	0.59 (0.52–0.67)	0.61 (0.53–0.69)	0.65 (0.57–0.73)	0.60 (0.52–0.68)	0.63 (0.55–0.72)	0.58 (0.50–0.67)	0.65 (0.57–0.73)
Deep vascular complex																		
Reference	0.262	0.455	0.443	0.472	0.480	0.472	0.453	0.456	0.470	0.262	0.455	0.443	0.472	0.480	0.472	0.453	0.456	0.470
Comparison	−0.020	0.013	0.024	−0.004	0.000	0.004	0.006	0.006	0.017	−0.005	−0.027	−0.012	−0.018	−0.018	−0.017	−0.023	−0.023	−0.021
Difference (%)	−7.6	2.9	5.4	−0.8	0.0	0.8	1.3	1.3	3.6	−1.9	−5.9	−2.7	−3.8	−3.8	−3.6	−5.1	−5.0	−4.5
P value	**0.017**	0.12	**0.004**	0.654	0.963	0.628	0.463	0.502	**0.042**	0.529	**< 0.001**	0.132	**0.028**	**0.027**	**0.044**	**0.006**	**0.006**	**0.012**
AUC (95% CI)	0.61 (0.53–0.69)	0.59 (0.52–0.67)	0.54 (0.47–0.61)	0.68 (0.61–0.75)	0.64 (0.56–0.72)	0.64 (0.56–0.72)	0.61 (0.53–0.69)	0.60 (0.52–0.68)	0.57 (0.49–0.65)	0.54 (0.45–0.62)	0.69 (0.63–0.76)	0.61 (0.54–0.69)	0.68 (0.61–0.75)	0.73 (0.67–0.79)	0.65 (0.58–0.73)	0.67 (0.59–0.75)	0.68 (0.60–0.75)	0.67 (0.60–0.75)

AUC = area under the receiver operating characteristic curve; CI = confidence interval.
Reference rows indicate the adjusted mean value of the OCT angiography metric in the control group, comparison rows indicate the estimated difference between the mean for the relevant group (diabetes mellitus and no diabetic retinopathy or diabetic retinopathy) and the control group mean. Comparisons between the control group and diabetes mellitus and diabetic retinopathy group with $P < 0.05$ appear in boldface. The AUC values are from models classifying diabetes mellitus and diabetic retinopathy status using OCT angiography metrics as the sole predictor.
*Adjusted for age, sex, hypertension, smoking status, and refractive error.

Table 4. Associations between OCT Angiography Foveal Avascular Zone and Whole Image Fractal Metrics and Diabetes Mellitus and Diabetic Retinopathy Status

Metric	Parameter Estimate	95% Confidence Interval	*P* Value	Area under the Receiver Operating Characteristic Curve	95% Confidence Interval
FAZ diameter minimum (mm)					
Reference	0.470	0.417–0.523	<0.001		
DM and no DR	0.015	−0.026 to 0.057	0.477	0.59	0.52–0.67
DR	0.004	−0.036 to 0.045	0.828	0.53	0.45–0.61
FAZ diameter maximum (mm)					
Reference	0.674	0.614–0.733	<0.001		
DM and no DR	−0.002	−0.051 to 0.047	0.935	0.53	0.45–0.62
DR	−0.017	−0.064 to 0.031	0.493	0.53	0.45–0.61
FAZ perimeter (mm)					
Reference	2.490	2.160–2.819	<0.001		
DM and no DR	−0.318	−0.601 to −0.036	**0.028**	0.59	0.51–0.66
DR	−0.358	−0.636 to −0.080	**0.012**	0.61	0.54–0.69
FAZ circularity					
Reference	0.627	0.555–0.698	<0.001		
DM and no DR	0.141	0.079–0.203	**<0.001**	0.71	0.64–0.79
DR	0.099	0.037–0.161	**0.002**	0.64	0.56–0.72
FAZ area (mm^2)					
Reference	0.223	−0.170 to 0.617	0.267		
DM and no DR	−0.058	−0.326 to 0.209	0.670	0.56	0.47–0.64
DM and DR	−0.048	−0.316 to 0.219	0.723	0.53	0.45–0.60
Fourier average fractal dimensions (slope)					
Reference	−1.987	−2.029 to −1.944	<0.001		
DR	0.037	0.002–0.073	**0.038**	0.59	0.50–0.68
DM and no DR	−0.022	−0.056 to 0.012	0.212	0.58	0.49–0.66
Multispectral fractal dimensions (slope)					
Reference	1.856	1.851–1.861	<0.001		
DM and no DR	0.001	−0.003 to 0.005	0.723	0.57	0.49–0.65
DR	−0.005	−0.009 to −0.001	**0.007**	0.61	0.53–0.69

DM = diabetes mellitus; DR = diabetic retinopathy; FAZ = foveal avascular zone.
Adjusted for age, sex, hypertension, smoking status, and refractive error. Reference rows indicate the adjusted mean value of the OCT angiography metric in the control group (i.e., the estimated model intercept). Other rows indicate the estimated difference between the mean for the relevant group and the control group mean. The area under the receiver operating characteristic curve values are from models classifying DM and DR status using OCT angiography metrics as the sole predictor. Boldface indicates statistical significance.

variation in normal foveal architecture that has been shown to be substantial,[34] and rarely correct for potential confounding variables. Most studies have reported an enlargement in FAZ diameter and area in eyes of persons with DM compared with control participants.[26–29] We found that the perimeter decreased in both DM groups compared with control participants, whereas the circularity increased, which is at odds with the findings of others. This may have arisen because we analyzed only the SVC, whereas others used the DVC, which is more likely to exhibit FAZ abnormalities early in the disease.[26,29] Our data also differ from reports that have provided the FAZ measurement from the inner retina slab that did not distinguish the SVC from the DVC.[27,28] Therefore, we contend that differences in segmentation and our choice of slab likely explain the differences that we observed.[35] However, our use of a large control population drawn from a cohort of community-based sampling and an older age group provides a better representation of the normal variation in foveal architecture, and therefore, differences that may have arisen by chance, particularly in studies with small sample sizes, are avoided.

Fractal analysis quantifies the complexity or density of the vessel branching pattern visible in a retinal image in terms of a fractal dimension and generates a single value that summarizes how complex or sparse the vascular pattern is. Variations in the fractal dimension are an indicator of deviation away from the normal or optimized network, and so a potential marker of disease. In multifractal analysis, the retinal vasculature is characterized as a spectrum of dimensions at different scales having first segmented the vessels. The measurement "fractal dimensions" in multifractal analysis is a metric ranging between 1 and 2, with higher values reflecting increased complexity of a vascular network. Although several studies have reported that fractal dimensions are altered in the presence of DR,[36,37] we found differences only in multispectral dimensions between control participants and those with manifest DR. Restricting analysis for FAZ to the SVC may have contributed to this finding, because others have reported greater effects seen in the DVC.[36]

Our data are the first to show subtle macular microcirculatory abnormalities in eyes with peripheral DR only. The importance of DR features in the peripheral retina has been shown to be an important predictor for worsening of DR.[19] Both

Table 5. Associations between OCT Angiography Metrics and Presence versus Absence of Diabetic Retinopathy in the Periphery

Slab	Adjusted for Age and Sex								Adjusted for Age, Sex, Hypertension, Smoking Status, and Refractive Error							
	C0	*I1*	*I2*	*N1*	*N2*	*S1*	*S2*	*T1*	*T2*	*C0*	*I1*	*I2*	*N1*	*N2*	*S1*	*S2*	*T1*	*T2*
Nerve fiber layer vascular plexus																		
Reference	−0.004	0.015	0.112	0.017	0.070	0.021	0.126	0.020	0.033	0.006	0.024	0.120	0.028	0.078	0.031	0.134	0.031	0.043
Comparison	−0.004	−0.004	−0.005	−0.011	−0.017	−0.004	−0.006	−0.009	−0.010	−0.003	−0.003	−0.008	−0.009	−0.019	−0.007	−0.022	−0.010	−0.011
P value	0.730	0.780	0.680	0.420	0.200	0.770	0.650	0.500	0.450	0.790	0.850	0.560	0.520	0.190	0.610	0.120	0.500	0.420
Superficial vascular complex																		
Reference	0.071	0.301	0.376	0.300	0.375	0.319	0.367	0.275	0.342	0.080	0.307	0.383	0.307	0.382	0.327	0.373	0.283	0.349
Comparison	−0.009	−0.004	−0.006	0.001	−0.006	−0.005	−0.030	−0.010	−0.036	−0.014	−0.001	−0.015	0.011	−0.005	−0.011	−0.044	−0.013	−0.044
P value	0.650	0.800	0.740	0.970	0.760	0.790	0.098	0.600	**0.048**	0.530	0.950	0.450	0.590	0.810	0.570	**0.028**	0.520	**0.027**
Deep vascular complex																		
Reference	0.248	0.453	0.453	0.454	0.467	0.462	0.446	0.447	0.472	0.276	0.482	0.481	0.482	0.495	0.490	0.473	0.476	0.501
Comparison	0.003	−0.007	−0.004	−0.009	−0.016	−0.038	−0.059	−0.038	−0.050	0.006	−0.003	−0.008	0.003	−0.001	−0.033	−0.061	−0.045	−0.057
P value	0.860	0.720	0.820	0.640	0.390	**0.045**	**0.002**	**0.047**	**0.009**	0.780	0.880	0.710	0.890	0.950	**0.110**	**0.004**	**0.034**	**0.007**

Reference rows indicate the adjusted mean value of the OCT angiography metric in the control group. Comparison rows indicate the estimated difference between the mean for the relevant group (diabetes mellitus and no diabetic retinopathy or diabetic retinopathy) and the control group mean. Comparisons between the control group and diabetes mellitus and diabetic retinopathy group with $P < 0.05$ appear in boldface.

the presence and extent of predominantly peripheral lesions were associated with an increased risk of progression of proliferative DR independent of baseline DR severity and hemoglobin A1c levels.[18,19] However, we recognize that the number of eyes with only peripheral lesions (n = 11) was very small, and therefore the results need to be interpreted accordingly. A recent comparison between severity of DR lesions using ultra-widefield imaging and OCTA in a larger sample used a predominantly peripheral lesions category, rather than exclusively peripheral lesions, in which lesions could be present in the ETDRS fields, although to a lesser extent. The study found a poor relationship between OCTA vessel density and DR severity and concluded that eyes with predominantly peripheral lesions had DR severity associated with primarily peripheral, rather than posterior, nonperfusion.[38] The differences in categorization make direct comparisons difficult.

Among the strengths of this study is the use of data from a large control population because it is already known that a variety of factors beyond retinal disease impact quantitative OCT parameters. Therefore, it is unlikely that matching using a 1:1 ratio for age would be sufficient to capture the natural variation in the general population. All participants originated from the population-based NICOLA study (https://nicola.qub.ac.uk/). This is an advantage compared with most clinical studies, which tend to recruit opportunistic control samples from university or hospital staff or their friends and family. The quality of a case-control study is contingent on the quality of the control population in terms of representativeness to the general population. The current study had a 1:4 case-to-control ratio, which from a statistical standpoint is considered optimal in terms of the precision of parameter estimates.[39] We also controlled for the main known confounders of OCTA quantitative parameters (age,[40] hypertension,[14] smoking status,[41,42] and refractive error[43]). The relatively wide normal variation of parameters among the control participants even after correction for known confounders is reflected in the lower AUC than reported in other studies.[44,45] The study also benefits from the characterization of DR using multimodal retinal imaging in addition to OCTA and the characterization of DR in the periphery using Optomap imaging using standardized reading center protocols.

Several weaknesses in the study are also worth considering when interpreting the results. Looking for differences among 9 segments and 3 layers results in a large number of comparisons being undertaken. Strict Bonferroni correction would require only those of less than 0.002 to be retained as statistically significant, which, it could be argued, is too conservative.[46] However, some of the comparisons barely reached the less than 0.05 threshold, hence, our focus on the effect sizes and directions of observed effects rather than the *P* values alone. The numbers of eyes with DR and in particular peripheral-only DR is very small and therefore may be underpowered to detect associations. This should be considered when interpreting the results. The initial assessment of quality of images was carried out by a single grader (R.E.H.) and no reliability metrics were assessed; however, general agreement with the machine-generated quality score and also eyes or segments in which the machine failed to return a density measurement because of poor quality provided confidence in the

assessment. We also were constrained to the segmentation slabs provided by the algorithm; other studies have suggested that the mid capillary plexus should be considered.[47]

In summary, significant differences in OCTA metrics can be found in those with DM before manifest DR using commercially available equipment with minimal image manipulation. Although diagnostic performance was poor, these metrics may be useful for measuring change over time in clinical trials. Longitudinal studies are warranted to explore further the usefulness of OCTA vessel metrics in clinical practice and interventional studies.

Acknowledgments

The authors thank all the participants of the NICOLA Study and the entire NICOLA team, which includes nursing staff, research scientists, clerical staff, computer and laboratory technicians, managers, and receptionists.

Footnotes and Disclosures

Originally received: February 19, 2021.
Final revision: May 13, 2021.
Accepted: May 20, 2021.
Available online: May 26, 2021. Manuscript no. D-21-00017.

[1] Centre for Public Health, Queen's University Belfast, Belfast, United Kingdom.

[2] Heidelberg Engineering GmbH, Heidelberg, Germany.

[3] Queen's Medical Research Institute, University of Edinburgh, Edinburgh, United Kingdom.

[4] School of Medicine, Tufts University, Boston, Massachusetts.

[5] Moorfields Eye Hospital, London, United Kingdom.

[6] University of Crete, Crete.

[7] School of Medicine, Louisiana State University, New Orleans, Louisiana.

Disclosure(s):
All authors have completed and submitted the ICMJE disclosures form.

The author(s) have made the following disclosure(s): R.E.H.: Consultant — Roche; Financial support — Novartis Optos Plc, UC Bayer
R.D.-M.: Consultant — Heidelberg Engineering GmbH, TM Optos plc
N.W.: Consultant — Apellis, Nidek, Boehringer Ingelheim; Financial support — Carl Zeiss Meditec, Heidelberg, Nidek, Optovue, Topcon, Regeneron; Equity owner — Ocudyne; Board member — Gyroscope Therapeutics
M.M.T.: Employee — Heidelberg Engineering GmbH
B.M.: Financial support — Alzheimer's Society, ESRC, NIA, HSC R&D, Dunhill Medical Trust; Lecturer — Nutricia
T.M: Financial support — Diabetes UK
T.P.: Consultant — Bayer, Novartis, Heidelberg Engineering, Zeiss
U.C.: Consultant — Roche

Bayer partially funded the retinal grading via an unrestricted educational grant to Queen's University Belfast. The NICOLA Study is supported by the Atlantic Philanthropies, the Economic and Social Research Council, the UKCRC Centre of Excellence for Public Health Northern Ireland, the Centre for Ageing Research and Development in Ireland, the Office of the First Minister and Deputy First Minister, the Health and Social Care Research and Development Division of the Public Health Agency, the Wellcome Trust/Wolfson Foundation, and Queen's University Belfast. The NISA Study is supported by the College of Optometrists. Diabetes UK, the Macular Society, Guidedogs for the Blind, the Thomas Pocklington Trust, and the Belfast Association for the Blind. The Macular Society, College of Optometrists, and Diabetes UK funded individual researchers. The sponsors and funding organizations had no role in the design or conduct of this research. The authors alone are responsible for the interpretation of the data and any views or opinions presented are solely those of the authors and do not necessarily represent those of the NICOLA Study team.

HUMAN SUBJECTS: Human subjects were included in this study. The human ethics committees at Queen's University Belfast approved the study. All research adhered to the tenets of the Declaration of Helsinki. All participants provided informed consent.

No animal subjects were included in this study.

Author Contributions:

Conception and design: Hogg, Wright, Dolz-Marco, Gray, Waheed, Teussink, Naskas, Perais, Das, Quinn, Bontzos, Nicolaou, Annam, Young, Kee, McGuiness, Mc Kay, MacGillivray, Peto, Chakravarthy

Analysis and interpretation: Hogg, Wright, Dolz-Marco, Gray, Waheed, Teussink, Naskas, Perais, Das, Quinn, Bontzos, Nicolaou, Annam, Young, Kee, McGuiness, Mc Kay, MacGillivray, Peto, Chakravarthy

Data collection: Hogg, Wright, Dolz-Marco, Gray, Waheed, Teussink, Naskas, Perais, Das, Quinn, Bontzos, Nicolaou, Annam, Young, Kee, McGuiness, Mc Kay, MacGillivray, Peto, Chakravarthy

Obtained funding: Hogg, Waheed, McGuiness, MacGillivray; Study was performed as part of the authors' regular employment duties. No additional funding was provided.

Overall responsibility: Hogg, Wright, Dolz-Marco, Gray, Waheed, Teussink, Naskas, Perais, Das, Quinn, Bontzos, Nicolaou, Annam, Young, Kee, McGuiness, Mc Kay, MacGillivray, Peto, Chakravarthy

Abbreviations and Acronyms:
AUC = area under the receiver operating characteristic curve; **DM** = diabetes mellitus; **DR** = diabetic retinopathy; **DVC** = deep vascular plexus; **ETDRS** = Early Treatment Diabetic Retinopathy Study; **FAZ** = foveal avascular zone; **NFLVP** = nerve fiber layer vascular plexus; **NICOLA** = Northern Ireland Cohort Study for the Longitudinal Study of Aging; **OCTA** = OCT angiography; **SVC** = superficial vascular plexus.

Keywords:
Diabetes mellitus, Diabetic retinopathy, Foveal avascular zone, OCTA, OCT angiography, Retinal periphery, Vessel density, Vessel segmentation.

Correspondence:
Ruth E. Hogg, PhD, Institute of Clinical Sciences, Block A, Centre for Public Health, Queen's University Belfast, Belfast BT12 6BA, United Kingdom. E-mail: r.e.hogg@qub.ac.uk.

References

1. Ting DS, Cheung GC, Wong TY. Diabetic retinopathy: global prevalence, major risk factors, screening practices and public health challenges: a review. *Clin Exp Ophthalmol*. 2016;44(4):260–277.
2. Kuwabara T, Cogan DG. Retinal vascular patterns. VI. Mural cells of the retinal capillaries. *Arch Ophthalmol*. 1963;69:492–502.
3. Kohner EM, Hamilton AM, Saunders SJ, et al. The retinal blood flow in diabetes. *Diabetologia*. 1975;11(1):27–33.

4. Kohner EM. The problems of retinal blood flow in diabetes. *Diabetes*. 1976;25(2 suppl):839−844.
5. Riva CE, Grunwald JE, Sinclair SH, et al. Blood velocity and volumetric flow rate in human retinal vessels. *Invest Ophthalmol Vis Sci*. 1985;26(8):1124−1132.
6. Mendivil A, Cuartero V, Mendivil MP. Ocular blood flow velocities in patients with proliferative diabetic retinopathy and healthy volunteers: a prospective study. *Br J Ophthalmol*. 1995;79(5):413−416.
7. Wang Y, Bower BA, Izatt JA, et al. In vivo total retinal blood flow measurement by Fourier domain Doppler optical coherence tomography. *J Biomed Opt*. 2007;12(4):041215.
8. Pinhas ADM, Shah N, Chui TY, et al. In vivo imaging of human retinal microvasculature using adaptive optics scanning light ophthalmoscope fluorescein angiography. *Biomed Opt Express*. 2013;4:1305−1317.
9. Palochak CMA, Lee HE, Song J, et al. Retinal blood velocity and flow in early diabetes and diabetic retinopathy using adaptive optics scanning laser ophthalmoscopy. *J Clin Med*. 2019;8(8):1165.
10. de Carlo TE, Romano A, Waheed NK, et al. A review of optical coherence tomography angiography (OCTA). *Int J Retina Vitreous*. 2015;1:5.
11. Tey KY, Teo K, Tan ACS, et al. Optical coherence tomography angiography in diabetic retinopathy: a review of current applications. *Eye Vis (Lond)*. 2019;6:37.
12. Sambhav K, Grover S, Chalam KV. The application of optical coherence tomography angiography in retinal diseases. *Surv Ophthalmol*. 2017;62(6):838−866.
13. Barraso M, Ale-Chilet A, Hernandez T, et al. Optical coherence tomography angiography in type 1 diabetes mellitus. Report 1: diabetic retinopathy. *Transl Vis Sci Technol*. 2020;9(10):34.
14. Sun C, Ladores C, Hong J, et al. Systemic hypertension associated retinal microvascular changes can be detected with optical coherence tomography angiography. *Sci Rep*. 2020;10(1):9580.
15. Cole ED, Ferrara D, Novais EA, et al. Clinical trial endpoints for optical coherence tomography angiography in neovascular age-related macular degeneration. *Retina*. 2016;36(suppl 1): S83−S92.
16. Spaide RF, Fujimoto JG, Waheed NK. Image artifacts in optical coherence tomography angiography. *Retina*. 2015;35(11): 2163−2180.
17. Croft DE, van Hemert J, Wykoff CC, et al. Precise montaging and metric quantification of retinal surface area from ultra-widefield fundus photography and fluorescein angiography. *Ophthalmic Surg Lasers Imaging Retina*. 2014;45(4):312−317.
18. Silva PS, Cavallerano JD, Sun JK, et al. Peripheral lesions identified by mydriatic ultrawide field imaging: distribution and potential impact on diabetic retinopathy severity. *Ophthalmology*. 2013;120(12):2587−2595.
19. Silva PS, Cavallerano JD, Haddad NM, et al. Peripheral lesions identified on ultrawide field imaging predict increased risk of diabetic retinopathy progression over 4 years. *Ophthalmology*. 2015;122(5):949−956.
20. Stosic T, Stosic BD. Multifractal analysis of human retinal vessels. *IEEE Trans Med Imaging*. 2006;25(8):1101−1107.
21. Kim AY, Chu Z, Shahidzadeh A, et al. Quantifying microvascular density and morphology in diabetic retinopathy using spectral-domain optical coherence tomography angiography. *Invest Ophthalmol Vis Sci*. 2016;57(9): OCT362−OCT370.
22. Nesper PL, Roberts PK, Onishi AC, et al. Quantifying microvascular abnormalities with increasing severity of diabetic retinopathy using optical coherence tomography angiography. *Invest Ophthalmol Vis Sci*. 2017;58(6):BI0307−BI015.
23. Zhang B, Chou Y, Zhao X, et al. Early detection of microvascular impairments with optical coherence tomography angiography in diabetic patients without clinical retinopathy: a meta-analysis. *Am J Ophthalmol*. 2021;222:226−237.
24. Rosen RB, Andrade Romo JS, Krawitz BD, et al. Earliest evidence of preclinical diabetic retinopathy revealed using optical coherence tomography angiography perfused capillary density. *Am J Ophthalmol*. 2019;203:103−115.
25. Thompson IA, Durrani AK, Patel S. Optical coherence tomography angiography characteristics in diabetic patients without clinical diabetic retinopathy. *Eye (Lond)*. 2019;33(4): 648−652.
26. Freiberg FJ, Pfau M, Wons J, et al. Optical coherence tomography angiography of the foveal avascular zone in diabetic retinopathy. *Graefes Arch Clin Exp Ophthalmol*. 2016;254(6): 1051−1058.
27. Mastropasqua R, Toto L, Mastropasqua A, et al. Foveal avascular zone area and parafoveal vessel density measurements in different stages of diabetic retinopathy by optical coherence tomography angiography. *Int J Ophthalmol*. 2017;10(10):1545−1551.
28. Lu Y, Simonett JM, Wang J, et al. Evaluation of automatically quantified foveal avascular zone metrics for diagnosis of diabetic retinopathy using optical coherence tomography angiography. *Invest Ophthalmol Vis Sci*. 2018;59(6):2212−2221.
29. Tarassoly K, Miraftabi A, Soltan Sanjari M, et al. The relationship between foveal avascular zone area, vessel density, and cystoid changes in diabetic retinopathy: an optical coherence tomography angiography study. *Retina*. 2018;38(8):1613−1619.
30. Mirshahi A, Ghassemi F, Fadakar K, et al. Effects of panretinal photocoagulation on retinal vasculature and foveal avascular zone in diabetic retinopathy using optical coherence tomography angiography: a pilot study. *J Curr Ophthalmol*. 2019;31(3):287−291.
31. Niestrata-Ortiz M, Fichna P, Stankiewicz W, et al. Enlargement of the foveal avascular zone detected by optical coherence tomography angiography in diabetic children without diabetic retinopathy. *Graefes Arch Clin Exp Ophthalmol*. 2019;257(4):689−697.
32. Greig EC, Brigell M, Cao F, et al. Macular and peripapillary OCTA metrics predict progression in diabetic retinopathy: a sub-analysis of TIME-2b Study data. *Am J Ophthalmol*. 2020;219:66−76.
33. Li X, Xie J, Zhang L, et al. Identifying microvascular and neural parameters related to the severity of diabetic retinopathy using optical coherence tomography angiography. *Invest Ophthalmol Vis Sci*. 2020;61(5):39.
34. Nolan JM, Stringham JM, Beatty S, et al. Spatial profile of macular pigment and its relationship to foveal architecture. *Invest Ophthalmol Vis Sci*. 2008;49(5):2134−2142.
35. Sacconi R, Borrelli E, Querques G. Reproducibility of vessel density, fractal dimension, and foveal avascular zone using 7 different optical coherence tomography angiography devices. *Am J Ophthalmol*. 2018;192:252−253.
36. Bhardwaj S, Tsui E, Zahid S, et al. Value of fractal analysis of optical coherence tomography angiography in various stages of diabetic retinopathy. *Retina*. 2018;38(9):1816−1823.
37. Zahid S, Dolz-Marco R, Freund KB, et al. Fractal dimensional analysis of optical coherence tomography angiography in eyes with diabetic retinopathy. *Invest Ophthalmol Vis Sci*. 2016;57(11):4940−4947.
38. Ashraf M, Sampani K, Rageh A, et al. Interaction between the distribution of diabetic retinopathy lesions and the association of optical coherence tomography angiography scans with diabetic

retinopathy severity. *JAMA Ophthalmol*. 2020;138(12):1291–1297.
39. Hamajima N, Hirose K, Inoue M, et al. Case-control studies: matched controls or all available controls? *J Clin Epidemiol*. 1994;47(9):971–975.
40. Jo YH, Sung KR, Shin JW. Effects of age on peripapillary and macular vessel density determined using optical coherence tomography angiography in healthy eyes. *Invest Ophthalmol Vis Sci*. 2019;60(10):3492–3498.
41. Ciesielski M, Rakowicz P, Stopa M. Immediate effects of smoking on optic nerve and macular perfusion measured by optical coherence tomography angiography. *Sci Rep*. 2019;9(1):10161.
42. Ayhan Z, Kaya M, Ozturk T, et al. Evaluation of macular perfusion in healthy smokers by using optical coherence tomography angiography. *Ophthalmic Surg Lasers Imaging Retina*. 2017;48(8):617–622.
43. Leng Y, Tam EK, Falavarjani KG, et al. Effect of age and myopia on retinal microvasculature. *Ophthalmic Surg Lasers Imaging Retina*. 2018;49(12):925–931.
44. Kaizu Y, Nakao S, Arima M, et al. Flow density in optical coherence tomography angiography is useful for retinopathy diagnosis in diabetic patients. *Sci Rep*. 2019;9(1):8668.
45. Ashraf M, Nesper PL, Jampol LM, et al. Statistical model of optical coherence tomography angiography parameters that correlate with severity of diabetic retinopathy. *Invest Ophthalmol Vis Sci*. 2018;59(10):4292–4298.
46. Perneger TV. What's wrong with Bonferroni adjustments. *BMJ*. 1998;316(7139):1236–1238.
47. Onishi AC, Nesper PL, Roberts PK, et al. Importance of considering the middle capillary plexus on OCT angiography in diabetic retinopathy. *Invest Ophthalmol Vis Sci*. 2018;59(5):2167–2176.